Electronic Supplementary Material (ESI) for Journal of Materials Chemistry A.

Supplementary Information

Following the In-plane Disorder of Sodiated Hard Carbon through *Operando* Total Scattering

Jette K. Mathiesen,[a,b] Ronald Väli,[c] Meelis Härmas, [c] Enn Lust,[c] Jon Fold von Bülow [d] , Kirsten M. Ø. Jensen[a*] and Poul Norby [b*]

[a] Department of Chemistry and Nanoscience Center, University of Copenhagen, DK-2100 Copenhagen Ø, Department of Energy Conversion and Storage, [b] Technical University of Denmark, DK-4000 Roskilde, Institute of Chemistry, [c] Institute of Chemistry, University of Tartu, Ravila 14A, 50411, Tartu, Estonia, [d] Haldor Topsoe A/S, DK-2800 Kgs. Lyngby.

1. Experimental setup for synchrotron *operando* total scattering

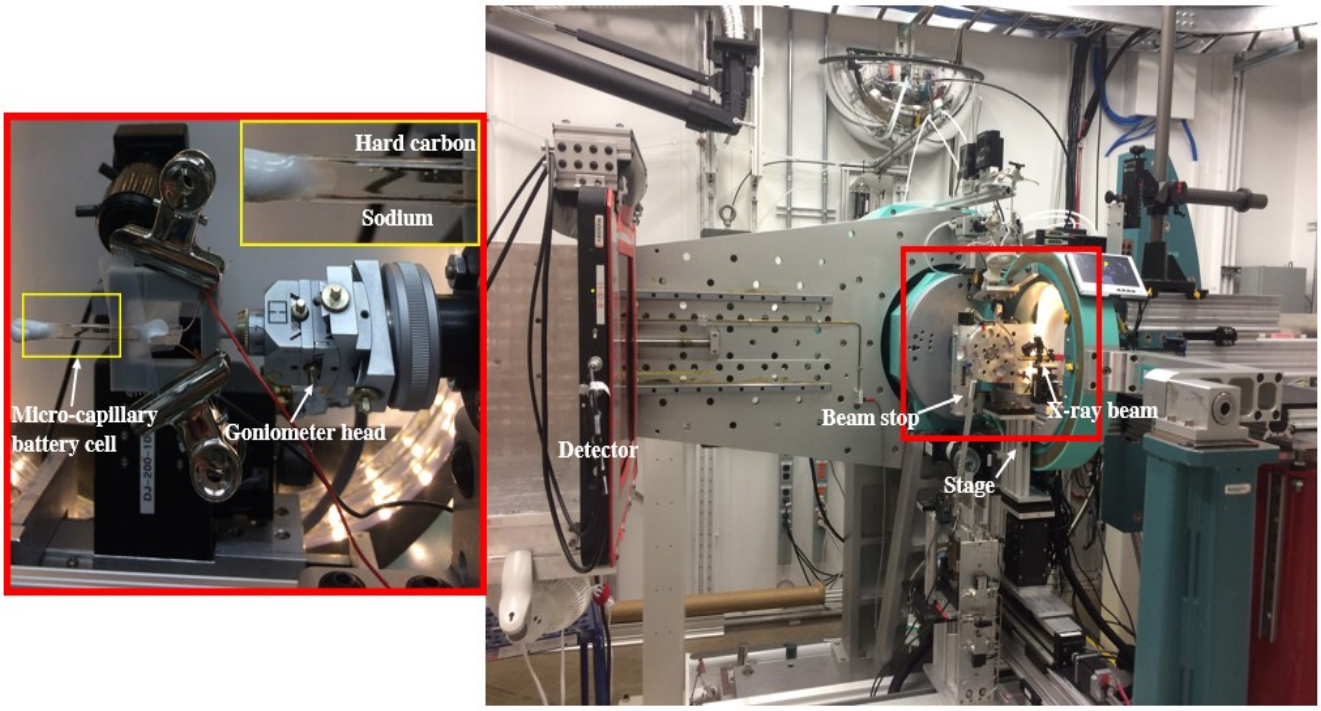

Figure S1. Experimental setup at beamline 11-ID-B, APS, for *operando* total scattering and PXRD measurements on micro-capillary battery cell.

2. Tabulated sequence of measurements

Table S1: Tabulated sequence of the measurements conducted during *operando* conditions.

Measurement	Position	Exposure time (minutes)
PDF	1	4.5
PDF	2	4.5
PDF (Background)	3	4.5
PDF	1	4.5
PDF	2	4.5

3. *Ex situ* PDF analysis of hard carbon

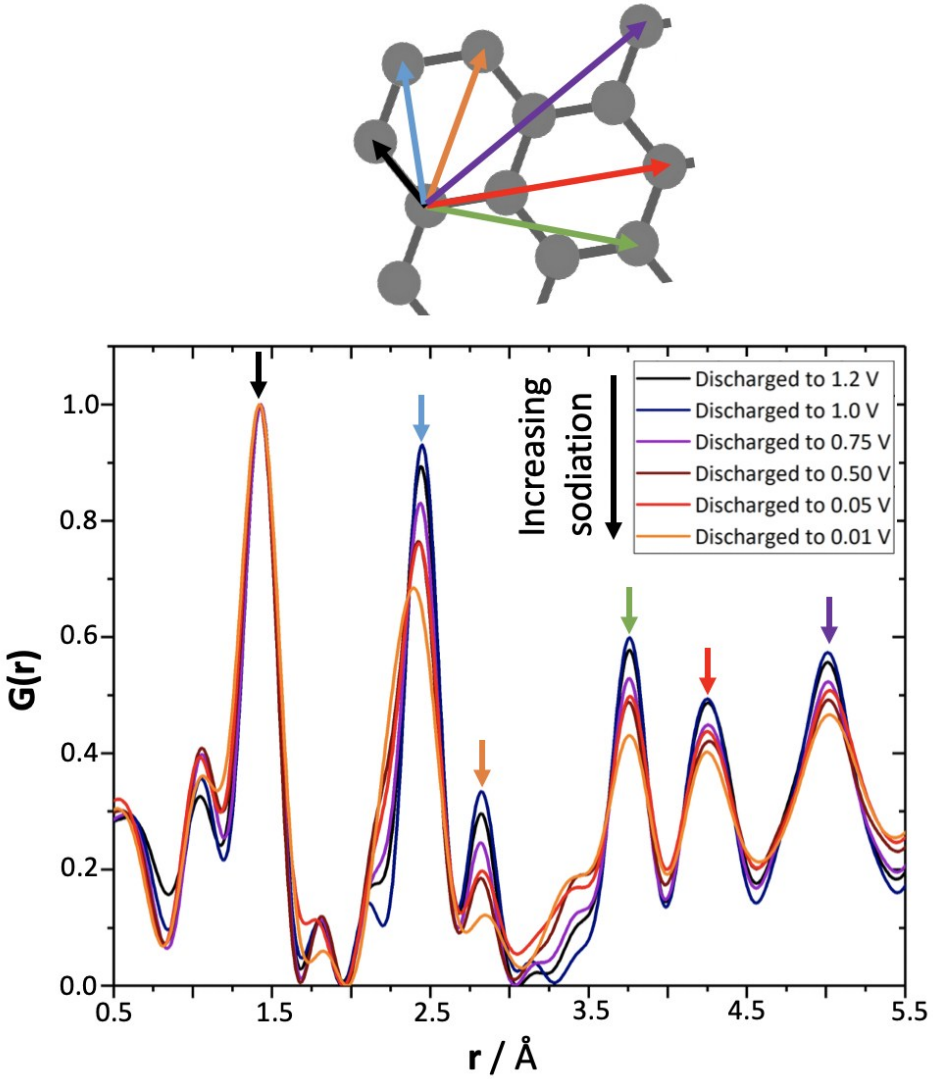

Figure S2 The G(r) of hard carbon at different sodiation stages indicating the correlations in a single graphene sheet (0.01 V designates the most sodiated stage).

Initial *ex situ* studies performed at P02, DESY, revealed that it was possible to index the C-C correlations within a single graphene sheet to the peaks in the PDF. In addition, it was observed that as the concentration of sodium increased in the hard carbon material, the peaks corresponding to C-C correlations across a single benzene ring became broader and therefore more disordered, which might originate due to a variation in C-C bond correlations

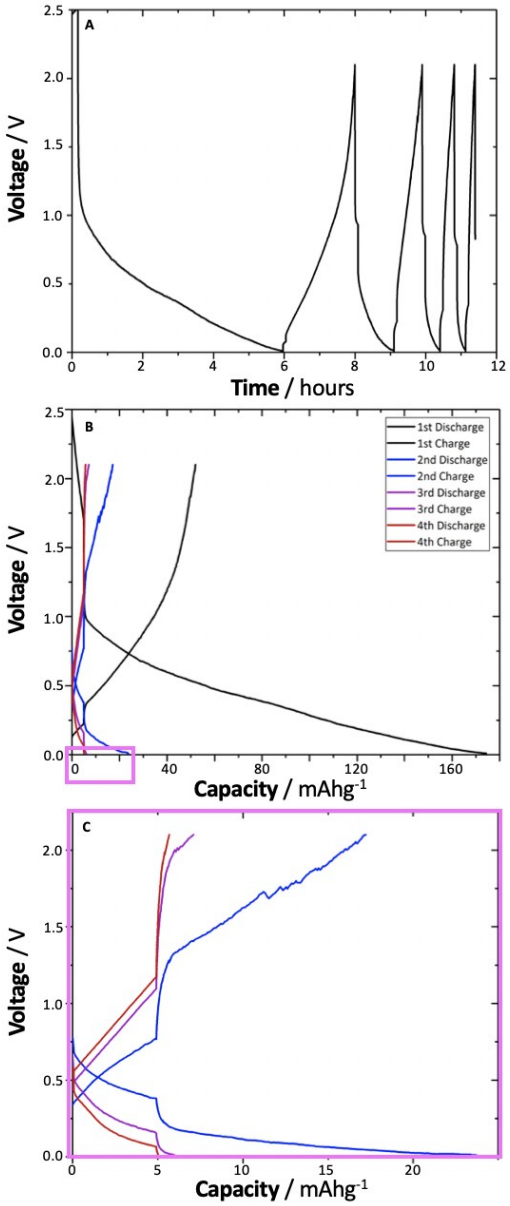

Figure S3 Electrochemical evaluation of hard carbon upon sodiation and de-sodiation. *A)* The galvanostatic cycling of the battery. *B)* Discharge-and charge capacities. *C)* The capacities of the 2nd to 4th cycles illustrating the large irreversible capacity loss.

4. Galvanostatic cycling of sodiation and de-sodiation of hard carbon with calculated capacities

The electrochemical galvanostatic cycling profile of hard carbon upon sodiation and de-sodiation is presented in Figure S5, where 5 minutes of OCV was performed in between discharge and charge for the cell to relax. A discharge capacity of 175 mAh/g was achieved with the micro-capillary cell, which is only 58% of the theoretical capacity (300 mAh/g, [2]). Furthermore, as the experiment is reversed upon charge, only a capacity of 52 mAh/g is observed corresponding to only 30% of the discharge capacity. As a further observation, the following cycles show extremely low discharge and charge capacities with the 3rd and 4th cycle only delivering 5 mAh/g upon discharge and charge (Figure S5C).

5. Refinement of hard carbon sodiation/de-sodiation

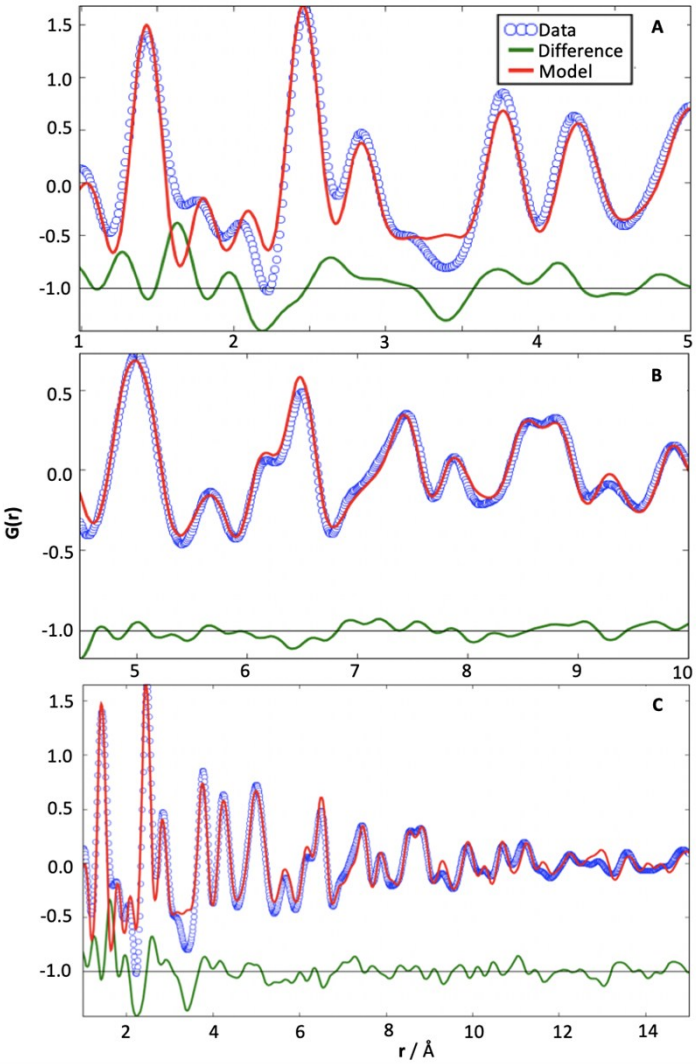

Figure S4 Refinement of first scan of hard carbon sodiation *A)* Low-r range refinement (1-5 Å), *B)* high-r range refinement (4.5-10 Å) and *C)* entire-r range refinement (1-15 Å).

The refinement was performed in PDFgui with a Qmax=20 Å, a spdiameter=25 Å (the particle diameter) and delta2 = 2 Å, taking into account correlated motion. If delta2 was refined, the values became negative upon refinement of the data. However, as this is unphysical, the parameter was fixed at a physically meaningful value. Upon the refinement, the U_{11} and U_{22} parameters of the U-matrix were constrained to refine with the same variable to simplify the model provided to the program and retain the symmetry in the graphite structure, whereas U_{33} was refined independently. Unit cell parameters, phase scale factor and the thermal parameters were all refined during refinements. The refinements were performed in three r-ranges: the low-r range from 1-5 Å, the high-r range from 4.5-10Å and the entire *r*-range from 1-15 Å, which are showed for the first scan in Figure S6.

6. Difference PDF

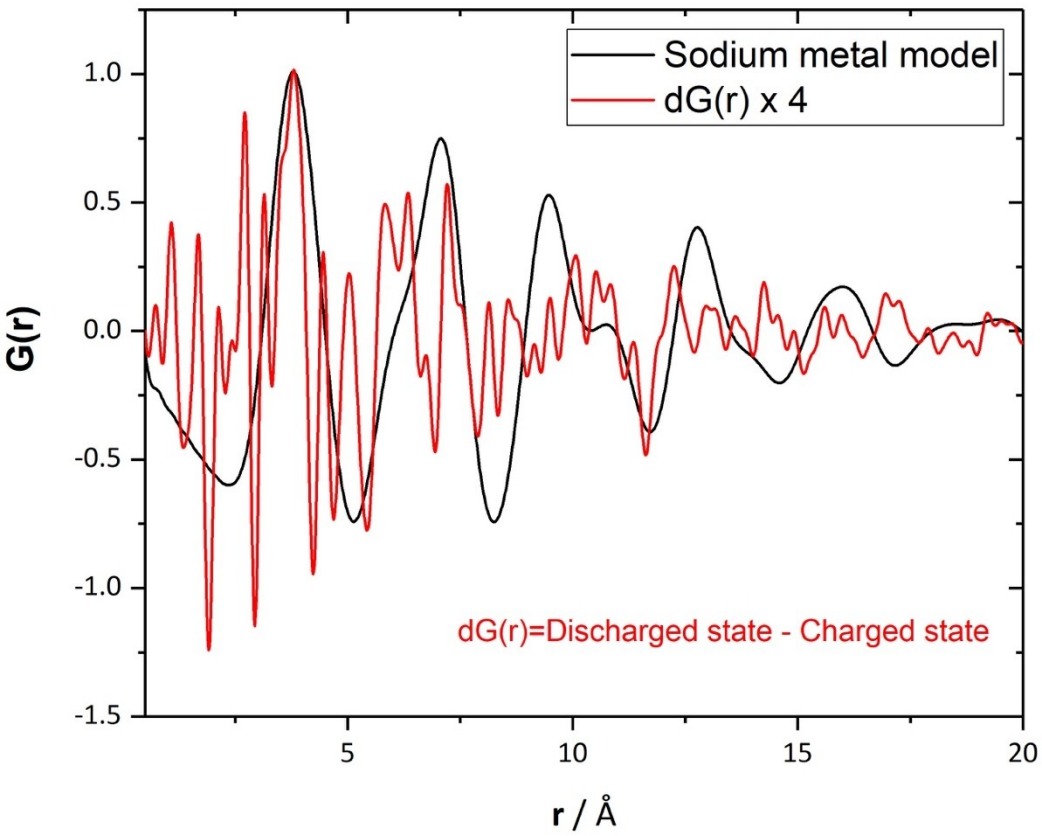

Figure S5 *Black curve)* Calculated PDF of sodium metal (No. 229). *Red curve)* Difference PDF between the experimental data at the fully discharged and charged states.

In Figure S6, a difference PDF plot between the discharged state and charged state is shown as the red curve. As the hard carbon structure and its graphene components are more pronounced in the charged state, six negative peaks are found at the positions of the graphene C-C correlation distances. The black curve in Figure S6 presents the calculated PDF of sodium metal with parameters provided by Grey et al. [1], where three peaks are illustrated. For comparison between the experimental difference PDF and sodium metal model, the difference PDF presented has been multiplied by 4 for scaling.

7. Galvanostatic cycling of lithiated hard carbon with calculated capacities

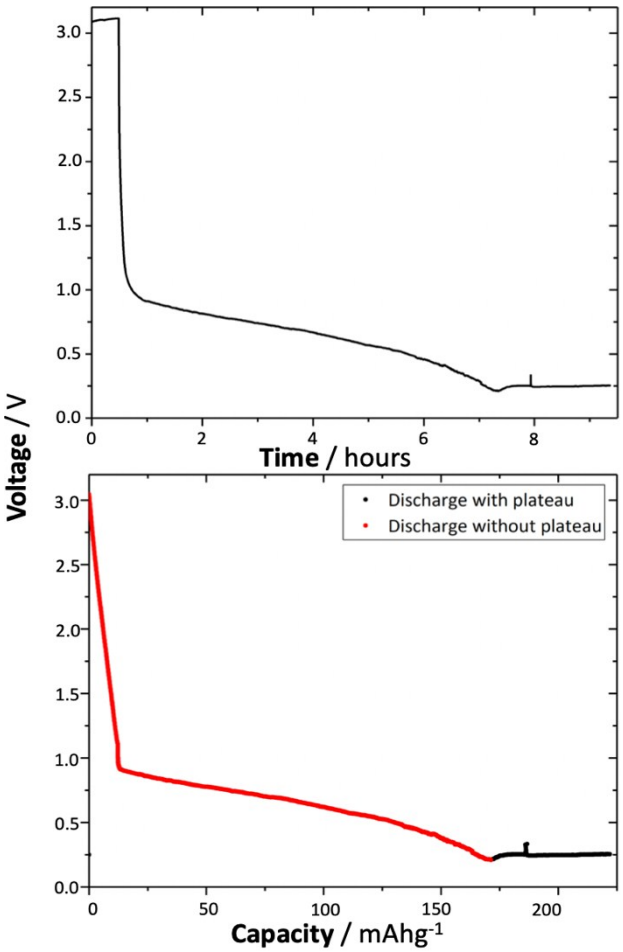

Figure S6 Electrochemical evaluation of hard carbon upon lithiation. *A)* The galvanostatic discharge of the battery. *B)* Discharge capacities, where the red curve corresponds to the capacity without the plateau and the black curve corresponds to the capacity with the plateau included.

The *operando* cell was cycled at a C-rate of C/10 with a current of 7.4 μA in the potential range 0.01-2.1 V. The electrochemical galvanostatic cycling profile of hard carbon upon lithiation and de-lithiation is presented in Figure S7A, where 5 minutes of OCV was performed in between discharge and charge for the cell to relax. As observed in Figure S7A, the same long discharge profile results as seen in the sodium system. However, as the system reached a voltage of 0.25 V, a plateau was reached, most probably due to unknown side-reactions. The battery was therefore stopped as it seemed to be stuck on this plateau. Furthermore, the galvanostatic cycling was suddenly interrupted as the potentiostat was disconnected. The battery was however still capable of reaching a discharge capacity of 171 mAh/g (222 mAh/g if plateau included), which corresponds to 68% (88% with plateau) of the theoretical discharge capacity (251 mAh/g, [3]). As no charge was initiated, the reversible character of the capacity cannot be examined.

8. Refinement of hard carbon lithiation

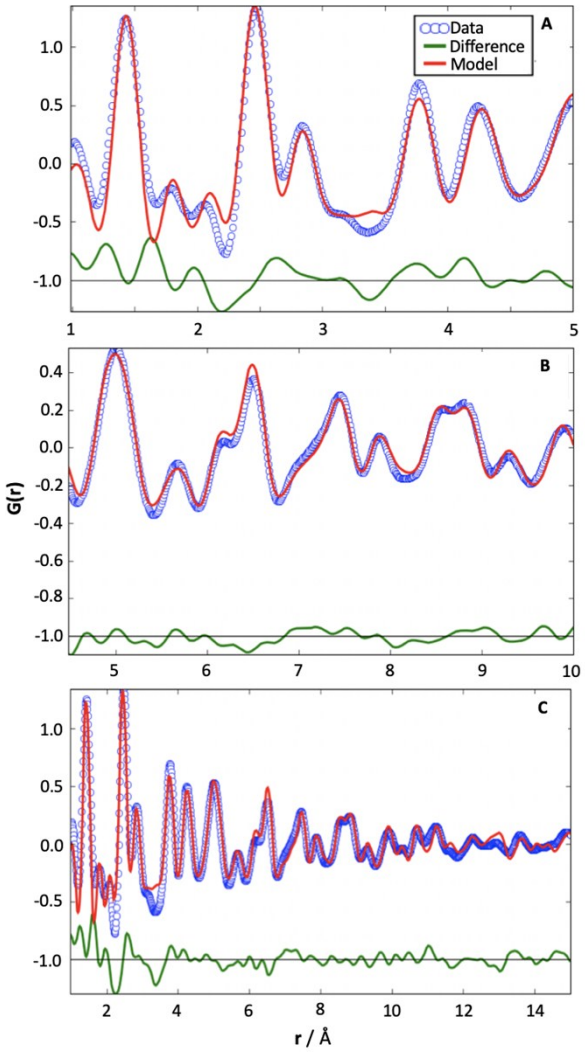

Figure S7 Refinement of first scan of hard carbon lithiation. *A)* Low-r range refinement (1-5 Å), *B)* high-r range refinement (4.5-10 Å) and *C)* entire-r range refinement (1-15 Å).

The refinement was performed in PDFgui with a Qmax=20 Å, a spdiameter=25 Å (the particle diameter) and delta2 = 2 Å, taking into account correlated motion. If delta2 was refined, the values became negative upon refinement of the data, which is, however, not physically meaningful. To overcome this, the parameter was fixed at a physically meaningful value. Upon the refinement, the U_{11} and U_{22} parameters of the U-matrix were constrained to refine with the same variable to simplify the model provided to the program and retain the symmetry in the graphite structure, whereas U_{33} was refined independently. Unit cell parameters, phase scale factor and the thermal parameters were all refined during refinements. The refinements were performed in three r-ranges: the low-r range from 1-5 Å, the high-r range from 4.5-10Å and the entire *r*-range from 1-15 Å, which are showed for the first scan in Figure S8.

9. Refinement of hard carbon lithiation

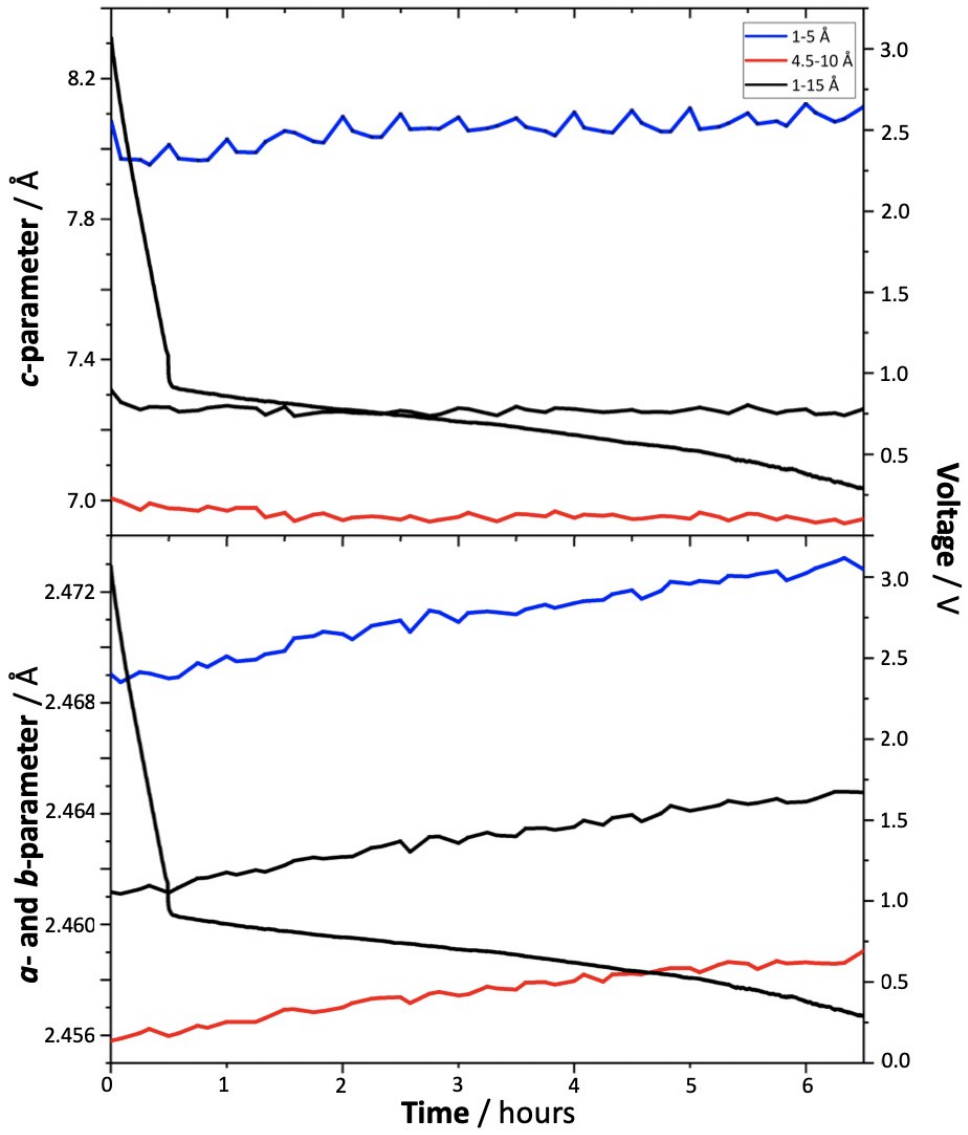

Figure S8 Refinement of *a*-, *b*- and *c*-parameter of the hard carbon structure upon lithiation in the three r-ranges of refinement as a function of the electrochemical state of charge. The state of charge of the half-cell is indicated as the black curve with corresponding cell voltage on the right of the figure.

References

[1] J. M. Stratford, P. K. Allan, O. Pecher, P. A. Chater, and C. P. Grey, *Chem. Commun.*, 2016, **52**, 12430-12433.
[2] Väli, R., Jänes, A., Thomberg, T., & Lust, E., *Journal of The Electrochemical Society*, 2016, **163**, A1619-A1626.
[3] Sun, X., Zhang, X., Liu, W., Wang, K., Li, C., Li, Z., & Ma, Y, *Electrochimica Acta*, 2017, **235**, 158-166.